Available online at www.sciencedirect.com

ScienceDirect

Procedia Manufacturing 11 (2017) 355 – 363

Procedia MANUFACTURING

27th International Conference on Flexible Automation and Intelligent Manufacturing, FAIM2017, 27-30 June 2017, Modena, Italy

The WIRES experiment: tools and strategies for robotized switchgear cabling

M. Busi[a], A. Cirillo[b], D. De Gregorio[c], M. Indovini[a], G. De Maria[b], C. Melchiorri[c], C. Natale[b], G. Palli[c]*, S. Pirozzi[b]

[a] *I.E.M.A. Srl, Via XXV Aprile 1945, 16, 40016 San Giorgio di Piano, Italy*
[b] *Università degli Studi della Campania "Luigi Vanvitelli", Viale Abramo Lincoln, 5, 81100 Caserta, Italy*
[c] *Università degli Studi di Bologna, Viale Risorgimento 2, 40136 Bologna, Italy*

Abstract

This paper presents the preliminary results obtained within the WIRES experiment. This experiment aims to automatize the switchgear wiring process by using industrial manipulators and properly designed hardware and software tools. The challenging objective of the experiment is the development of a proper computer vision algorithm able to detect the switchgear components and a novel gripper, with an integrated tactile sensor, able to manipulate wires and simultaneously operate on screw/clip type connection points. Another objective of the experiment is the development of a software package able to optimize the wiring sequence and to plan the robot trajectories, based on the CAD data coming from the switchgear design software. The concept of such a software tool is here presented.

Peer-review under responsibility of the scientific committee of the 27th International Conference on Flexible Automation and Intelligent Manufacturing

Keywords: Added Value Manufacturing, Tactile Sensors, Robotics, Dexterous Manipulation, Deformable Objects.

* Corresponding author. Tel.: +39-051 20 93 186
E-mail address: gianluca.palli@unibo.it

Peer-review under responsibility of the scientific committee of the 27th International Conference on Flexible Automation and Intelligent Manufacturing
doi:10.1016/j.promfg.2017.07.118

1. Introduction

Nomenclature

E	Young's modulus
d	wire diameter
δz_{ij}	mean vertical displacement of (i,j)-th cell ceiling
x_i^c	i-th row centroid
n	number of taxels for each row and column
L	length of one side of the sensor base
g (y)	function describing the actual wire shape
f (y)	function describing the estimated wire shape
μ	metric quantifying the error between the estimated wire shape and the actual one

Recently, the robotic systems integrate more and more often advanced end effectors for the successful execution of grasping and manipulation tasks. For these applications, the characteristics of the manipulated object are always collected by using vision and/or tactile sensors. In many research papers, the vision is used alone 0, [2], but it may fail in presence of occlusions and lighting variations. To overcome these limitations, additional information about object features can be acquired by using tactile sensors. Many researchers have been working on integrating vision and tactile data for object recognition for more than thirty years [3]. The objectives of more recent papers on this field concern: object pose estimation [4], object shape estimation [5], the combination of visual and tactile exploration procedures [6], estimation of surface features [7], map object surfaces [8], and object recognition by using a cross-modal approach [9].

The main objective of the WIRES experiment [10] is the robotized cabling of switchgears. The cabling process is a very challenging task, which can be divided into two main subtasks: the connection and the routing phases. To this aim, the robotic system will make use of a suitably designed end effector equipped with a vision system and a tactile sensor for the wire precise manipulation. Moreover, a computer vision system is need to detect the right position of the components into the switchgear. In this paper, the authors firstly present the mechatronic design of the end effector from the mechanical structure and kinematics point of view to the optimization of the integrated sensory system.

A couple of commercial solutions for automatic wiring are available on the market, all with their pros and cons. The SYNDY robotized wiring tool [11], is very expensive (about 100k€) and requires a relatively large space between the components to be connected, mainly because of the dimensions and the mobility requirements of the robot end effector, fact that limits its applicability to the wiring of ceiling lamps. Indeed, SYNDY is not suited to operate with a relatively large number of different wires or when the component density is too large, as in the case of a typical switchgear configuration, due to the absence of force/tactile sensors that does not allow to safely interact with the components and the other wires during the wiring process. Moreover, SYNDY also cut the wires at the requested length “online”, but it is restricted to work with wires of a single color at a time. Another solution is provided by the Kiesling Averex wiring [12], but is this case the applicability is limited mainly by the fixed orientation of the wire and the screw, by the limited maximum dimension of the cable the machine can handle, by the limited machine workspace and by the fact tact the switchgear panel should be mounted in horizontal position.

To solve the issues affecting current solutions, the WIRES end effector is equipped with a jaw and a torque-controlled screwdriver for tightening the electromechanical component connectors. The jaw can be moved independently for the screwdriver along 3 axes, for cable positioning and insertion into the connectors. The jaws are equipped with a purposely-designed tactile sensor to ease the detection of the cable pose and monitor the insertion force. Moreover, a 3D camera is mounted into the end effector for a close view to the switchgear components. Different simulations in suitable development environments have been carried out to optimize the design of each end-effector part. The end effector will be mounted on an industrial manipulator, and a 6-axis force/torque sensor in the wrist interface will be adopted to control the interaction force between the robot and the switchgear components during cable connections. The gripper is provided with the necessary degrees of freedom with respect to the screwdriver to allow the precise positioning of the wire while the screwdriver itself is in contact with the component to close the terminal and therefore finalize the connection. In this phase, the information provided by the tactile

sensor are exploited by the gripper controller to properly manipulate the wire, performing the insertion of the wire in the terminal and verifying the connection after the terminal has been tightened. The effectiveness of the end-effector design, of the wire manipulation approach and of the trajectory generation software will be tested by simulations in a 3D virtual environment, in which the robot, the switchgear and the wire models will be included.

In the narrow spaces available between the components of a switchgear, the use of a vision system only could not be sufficient to obtain the necessary accuracy, mainly due to occlusion and shadowing problems. Instead, a tactile sensor, directly integrated into the gripper, provides a continuous feedback during the task execution, which can be used alone or together with visual data by using sensor fusion techniques. In particular, for the tactile sensor Finite Element (FE) models have been implemented (by using COMSOL Multiphysics®) to simulate the contact between the sensor and the wire during a generic grasping. For the sensor deformable layer, different shapes (flat and hemispherical) and taxel distributions (4x4 and 5x5 arrays) have been modeled. The wire has been modeled as an object rigid with respect to the tactile sensor and with a cylindrical shape locally curved. A detailed FE analysis has been carried out by considering different grasping cases, by varying the wire curvature, diameters and its relative position with respect to the sensor reference frame. For each grasping case, the capability of the sensor in the reconstruction of the wire shape and position has been evaluated, by comparing the actual features of the wire and the estimated ones.

2. The vision system

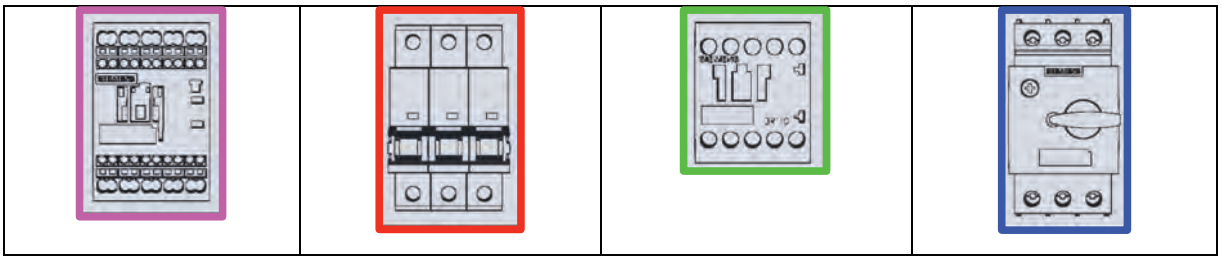

Fig. 1 - CAD Models of the electromechanical components.

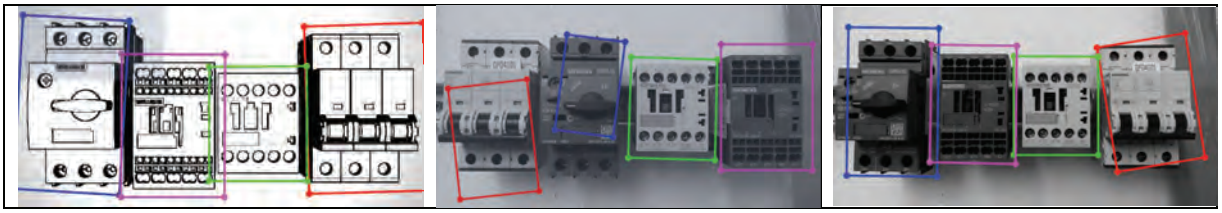

Fig. 2 - Scenes Matches using CAD models.

The main purpose of the vision system is to provide the location of the components mounted in the switchgear before executing the connections. Due to the large variety of components available and the continuous introduction into the market of new components, it is convenient to develop a vision system able to exploit the data provided by the component manufactures, and in particular the CAD design of the component itself. Moreover, since the component will be already mounted into the switchgear during the detection phase, only the frontal view can be considered for detection. Fig. 1 shows the frontal view of the component CAD design provided by the manufacturer for some sample components. The vision system will directly use this information for detecting the components on the switchgear. Fig. 2 reports some component detection tasks, in which a 3D CAD image and different real scenes with different lighting conditions are adopted. It is possible to see that the vision system is able to correctly detect the components in all the conditions.

First, we tested an algorithm dubbed BOLD [13], developed and patented by CVLAB (University of Bologna) that is able to detect and describe 2D Lines (Geometric Primitives) in images and perform good matches. Second, other Geometric Primitives like circles have been provided in BOLD to increase its performance in the Match stage. From the previous comparison of the performance of different component localization algorithms, the last proposed approach based on the BOLD algorithm using the CAD models of the component as feature models seems really

promising since it allows to exploit directly the CAD models, therefore avoiding the inclusion in the component database of images taken from the real component. Further improvements of this algorithm will be investigated to customize it for the particular problem at hand. A video showing the BOLD algorithm at work on a real scene can be seen in [14].

3. Extraction of the switchgear data from the CAD design

From the switchgear design software, it is possible to export the switchgear design data by means of spread sheets reporting all the components and related information, see Tab. 1. Moreover, the 3D model of the switchgear is exported in STEP or VRML format. The 3D switchgear model is of crucial importance for our purpose since it allows estimating the location of the components, the distance between them and the path and length of the cables. While the STEP format can be useful for 3D scene reconstruction and simulation, the VRML is very easy to process for extracting the switchgear information since it is a text file describing all the elements in the scene. Moreover, together with the VRML file, a text file (called WRI table) is also exported, which reports the links between the table with the component list shown above and the components name used in the VRML model in a hierarchical way as reported in Tab. 2. In this tables, a couple of different components have been highlighted in yellow and green respectively to show how the components into the component list can be linked to the VRML model by means of the WRI table. It is, then, clear that the data can be extracted and exploited for the generation of the manipulator trajectories directly by means of simple text elaboration and extraction libraries. Moreover, dedicated opensource software such as the OpenVRML C libraries can be exploited for manipulating the VRML data.

Tab. 1 - Example of switchgear component list.

Component Code	Article Num.	Quantity	Description	Commercial Code	Manufacturer	Destination
=-F0030.1	6502086	1	INT.AUT.1P 10A (C)	SIEMENS 5SY4110-7	SIEMENS	Q
=-F0030.1	6502088	1	CONTATTO AUX 1NO+1NC	SIEMENS 5ST3010	SIEMENS	Q
=-F0030.2	6502084	1	INT.AUT.1P 4A (C)	SIEMENS 5SY4104-7	SIEMENS	Q
=-F0030.2	6502088	1	CONTATTO AUX 1NO+1NC	SIEMENS 5ST3010	SIEMENS	Q
=-F1500.1	6503798	1	INT.AUT.3P 4,5..A	SIEMENS 3RV2011-1GA20	SIEMENS	Q
=-F1500.1	6503808	1	CONTATTO AUX 1NO+1NC	SIEMENS 3RV2901-2E	SIEMENS	Q

Tab. 2 - Connection between the WRI table (left) and the 3D model information from the VRML file (right).

```
…
ID000070   =-X1600              6012928
ID000071   =-Q1500.3  6503377
ID000072   =-Q1500.3  6503809
ID000073   =-U7                 WEI.TS35/15
ID000074   =-F1500.1  6503798
ID000075   =-F1500.1  6503808
ID000076   =-F1500.2  6503798
ID000077   =-F1500.2  6503808
ID000078   =-F1500.3  6503798
ID000079   =-F1500.3  6503808
ID000080   =-F0030.1  6502086
ID000081   =-F0030.1  6502088
ID000082   =-T0030              6032224
ID000083   =-F0030.2  6502084
ID000084   =-F0030.2  6502088
…
```

```
…
DEF ID000074 Transform {
        translation 112.500000 -0.500021 9.999981
        rotation -1.000000 0.000000 0.000000 1.570797
…
        geometry IndexedFaceSet {
                point [
        5.150000 -51.828000 -51.700000,
                                ….
DEF ID000083 Transform {
        translation 785.200000 0.000000 15.000000
        rotation 0.707107 0.707107 0.000000 3.141593
…
        geometry IndexedFaceSet {
                point [
        2.000000 26.210000 -35.857071,
…
```

4. Design of the WIRES end effector

The WIRES end effector includes an integrated torque/controlled screwdriver with remote PLC control and process data recording capabilities (Atlas Copco Tensor ETF SL21-04-l06), a Force/Torque sensor on the wrist interface (Schunk FTM75 Force-Torque Module), and it is composed by a couple of jaws that can be moved along three Cartesian axes to control the wire end position with respect to the screwdriver during the connection, as shown in

Fig. 3.

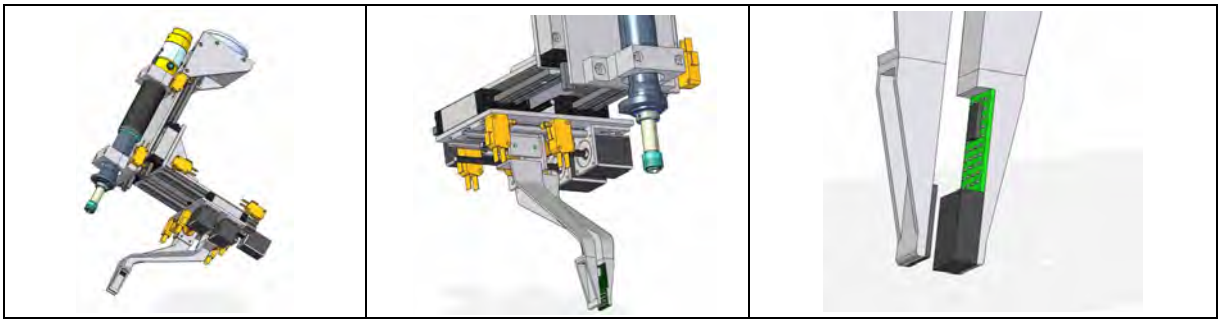

Fig. 3 - The WIRES end effector with integrated screwdriver and wrist force/torque sensor and detailed view of the tactile sensor.

Stepper motors with integrated encoder and lead screws have been adopted for the actuation of the end effector to simplify the control, reduce the weight, the mechanical complexity and the cost of the tool. Limit switches have been used for absolute position detection on both sides of all the end-effector movement axes.
The tactile sensor has been integrated into a jaw tip (fingertip) in such a way that different configurations can be evaluated during experiments. In fact, the fingertip can be easily substituted with a passive one (without tactile sensor) on one or both sides to save space or for preliminary tests. The CAD rendering of the fingertips reported in Fig. 3 shows a configuration with the tactile sensor on one side and a passive fingertip on the other side.
A conceptual view of the WIRES end effector integrated with an industrial manipulator is reported in the following pictures.

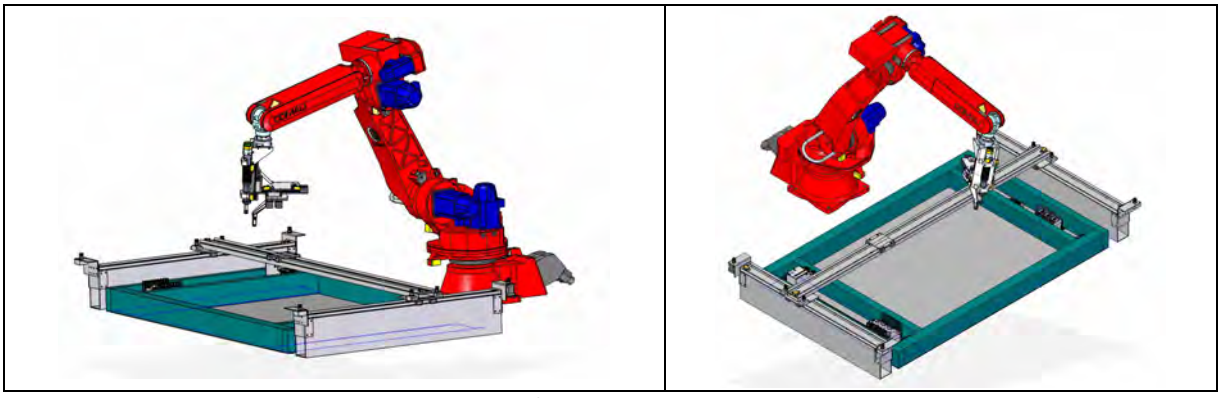

Fig. 4 – Overview of the WIRES robotized cabling system.

5. The tactile sensor

Starting from the tactile sensor working principle presented in [15], the authors will develop a version suitably optimized for wire manipulation. As in [15], the sensor is constituted by an optoelectronic layer and a deformable silicone layer. The optical taxels integrate a LED and a phototransistor (PT), while on the bottom side of the deformable layer there are empty cells, with ceilings on top of the optical components made of white silicone to enhance light reflection, while the walls separating the cells are black to avoid cross-talk effects. When an external force is applied to the deformable layer, it produces vertical displacements of the cell ceilings of all taxels. The distances between the white surfaces and the optical components change, producing variations of the reflected light and, in turn, of the PT photocurrents. According to the requirements of the switchgear cabling in terms of available space between switchgear components, the maximum allowed width for the tactile sensor is 20mm, while the maximum thickness is 7mm, well below the dimensions of the sensor in [15]. Since the wires have diameters of few millimeters, in addition to the dome shape, the solution with flat surface will be evaluated. In both cases, by considering the thickness of a standard Printed Circuit Board (PCB), the deformable layer can be realized with a

thickness of 5mm, complying with the assigned specification. Regarding the sensor width, to comply with the assigned specification, both 16 taxels, organized as a 4x4 matrix, and 25 taxels, organized as a 5x5 matrix can be considered. Hence, the design objective is to define the deformable layer shape and the number of taxels for the sensor to realize, on the basis of its capability in the reconstruction of the grasped wire shape.

5.1. The Finite Element analysis

Following the discussion above, by combining the two shapes (dome shaped and flat shaped) and the two taxel distributions (4x4 and 5x5), four different FE models have been implemented for the sensor design. The deformable layers have been modeled by using silicone (Young's modulus E=0.6MPa) as material and elements with tetrahedral shape for the meshes. The obtained models are constituted by the following number of elements: 8991 for the 4x4 flat shaped, 10821 for the 4x4 dome shaped. 12612 for the 5x5 flat shaped and 13860 for the 5x5 dome shaped. The grasped wire has been modeled as a rigid object, i.e., with a Young's modulus much higher than the one of the deformable layers. For all simulations a wire with diameter d = 4mm has been considered, since it is among the most commonly used wires in switchgears. A generic quadratic function has been used to model the shape of the wire. The obtained model, by using the same tetrahedral elements of the deformable layers, is characterized by a mesh of 1589 elements. Fig. 5 reports top views of the FE models for both dome shaped and flat shaped sensors, while Fig. 6 shows the bottom sides for both 4x4 and 5x5 taxel distributions. The models have been used to simulate the contact between the wire and the sensors by using the penalty method. The deformable layers are fixed constrained at the base. A prescribed displacement along the z-axis is applied to the wire, which comes into contact with the sensor.

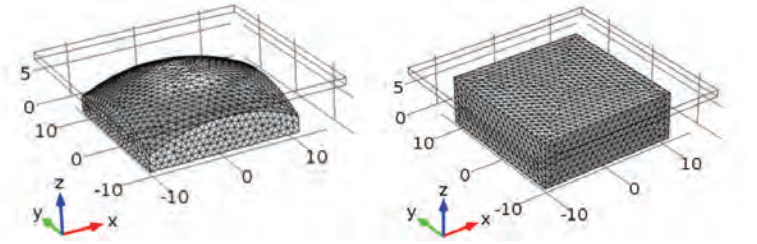

Fig. 5 - FE models with dome shape (left) and flat shape (right) (all dimensions are in mm).

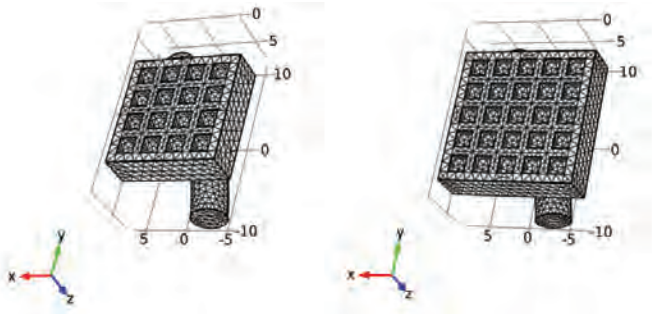

Fig. 6 - FE models with 4x4 (left) and 5x5 (right) taxel distribution (all dimensions are in mm).

The results of a generic simulation of the 5x5 flat shaped sensor are reported in Fig. 7. The wire is subject to a vertical displacement of 0.5mm. At the end of the simulation, the extracted data are the vertical displacements of the elements corresponding to the ceilings of the cells for all taxels. Fig. 7 shows how the wire shape is related to these vertical displacements, and, in particular, the subfigure on right highlights how the cells immediately under the wire shape show greater displacements than the lateral ones. More in detail, the optical component couples are sensitive to these vertical deformations and the voltage signal variations acquired from PTs can be assumed proportional to the mean vertical displacement δz_{ij} of the corresponding cell ceiling (where i and j represent row and column indices of the taxels, respectively).

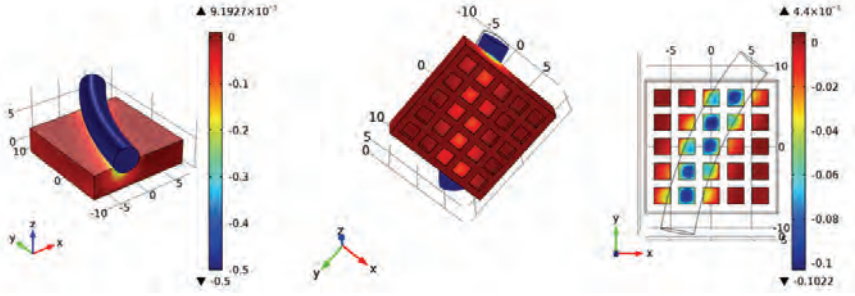

Fig. 7 - Vertical displacement for a generic simulation of the 5x5 flat shaped sensor: (left) top view, (middle) bottom view and (right) details of vertical displacements of the cell ceilings with zoomed in scale (all dimensions are in mm).

Hence, to evaluate sensor capabilities in the wire shape estimation, the mean vertical displacements δz_{ij} of the taxels are extracted for each simulated configuration. Each δz_{ij} value can be associated with the physical (x,y)-coordinates of the geometric center of the (i,j)-th cell. By graphically representing the mean vertical displacement of the (i,j)-th taxel as a circle with the center coincident with the physical (x,y)-coordinates of the cell center and the radius proportional to δz_{ij} value, a tactile map as reported in Fig. 8 (left) can be extracted from each simulation. Fig. 8 reports the tactile map for a 5x5 flat shape model. As described above the wire axis shape along the grasping area is modeled as a quadratic function. Let us assume to know if the wire longitudinal direction mainly lies along the x or y axis, since the wire is grasped by the robot in a known position. Since these two possible cases are similar from FE analysis point of view, only the case with the wire longitudinal direction lying along the y axis (as the case shown in Fig. 8) has been considered. The other case can be obtained as the dual case, swapping x and y axes in the following discussion. In the considered case, the generic wire shape to reconstruct can be expresses as

$$f(y) = ay^2 + by + c \tag{1}$$

whose parameters (a,b,c) have to be estimated from the vertical displacement δz_{ij} values. The proposed algorithm is:

- ✓ for each i-th row, the row centroid x_i^c is computed as

$$x_i^c = \frac{\sum_{j=1}^{n} x_j \delta z_{ij}}{\sum_{j=1}^{n} \delta z_{ij}} \quad i = 1,\mathrm{K}\ ,n \tag{2}$$

  where x_j represents the x-coordinate of the j-th column and n is the number of taxels for each row and column (n=4 or n=5 for the 4x4 and the 5x5 sensor, respectively);

- ✓ for each i-th row the centroid coordinates (x_c^i, y_i), with i=1,...,n, are defined, where y_i represents the y-coordinate of the i-th row;
- ✓ the function parameters (a,b,c) for the estimated wire shape are computed by using a least square method applied to the data set constituted by all row centroids.

By applying the proposed procedure to the tactile map reported in Fig. 8 (left), the row centroids highlighted as black markers have been computed. The obtained points have been used to estimate the quadratic function parameters (and, consequently, the estimated wire shape) reported in Fig. 8 (right). The figure shows a good matching between the estimated wire shape and the actual one. The matching quality can be quantified by computing, as reconstruction error, the following metric quantifying the error between the estimated wire shape f(y) and the function g(y) representing the actual wire shape

$$\mu = 1/L \int_{-L/2}^{L/2} \left| f(y) - g(y) \right| dy \tag{3}$$

where L is the side length of the sensor square base. For the case reported in Fig. 8, it is μ=0.38mm.

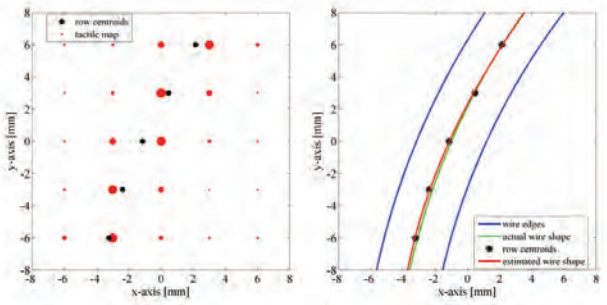

Fig. 8 - Grasped wire shape reconstruction for a generic simulation of the 5x5 flat shape: (left) tactile map with estimated row centroids and (right) estimated wire shape with respect to the actual one (all dimensions are in mm).

5.2. The comparison among the different cases

The algorithm described in the previous section has been applied to compare the reconstruction capabilities of the four sensors considered for the optimization: 4x4 dome shaped, 4x4 flat shaped, 5x5 dome shaped and 5x5 flat shaped. For all models contact cases with the wire in various configurations have been considered. Simulation results have been elaborated and the comparison between the estimated wire shape and the actual one has been evaluated by computing μ as defined in Eq. (3). The results, reported in Tab. 3, demonstrate that flat sensors have lower reconstruction errors, being μ always lower than the domed cases. The 5x5 flat sensor shows the lowest errors, but the differences with respect to the 4x4 flat sensor are minimal. As a consequence, the greater constructive complexity, that the 5x5 case presents with respect to the 4x4 case, makes the 4x4 flat sensor the best candidate for the realization within the WIRES experiment.

Tab. 3 - Comparison between considered sensors in various contact conditions.

	Reconstruction error μ for the considered sensors [mm]			
Contact configurations	5x5 flat shaped	4x4 flat shaped	5x5 dome shaped	4x4 dome shaped
	0.38	0.39	0.48	0.51
	0.37	0.39	0.45	0.50
	0.39	0.41	0.44	0.50
	0.40	0.41	0.48	0.51
	0.42	0.42	0.50	0.53
	0.40	0.41	0.49	0.52

6. Conclusions

The tools developed for the execution of the WIRES experiment have been presented in this paper. The 3D vision

system has been tested using only the information provided by the components manufacturer, and the data for the execution of the switchgear cabling have been extracted from the data exported by the switchgear design platform. Moreover, an end effector has been purposely designed for manipulating the electric cables and executing the connections on the switchgear electromechanical components.
The tactile sensor simulations demonstrated that the use of a deformable layer with a flat shape guarantees a better reconstruction of the grasped wire shape with respect to a dome shaped sensor. In addition, the use of a higher number of taxels can improve the quality of the estimated wire shape. However, the differences between the 4x4 and the 5x5 considered cases are minimal. Since the realization of a 5x5 tactile sensor needs a more complex PCB (with a higher number of routing layers and of Analog to Digital channels), the solution with 4x4 taxels and flat shaped will be realized for the WIRES experiment.

Acknowledgements

This work was supported by the European Commission Seventh Framework Programme (FP7/2007-2013) under grant agreement no. 601116 (ECHORD++ project - WIRES Experiment).

References

[1] A. Saxena, J. Driemeyer, and A. Y. Ng ”Robotic grasping of novel objects using vision”, The International Journal of Robotics Research, vol. 27(2), pp. 157-173, 2008.
[2] M. Popovic, D. Kraft, L. Bodenhagen, E. Baseski, N. Pugeault, D. Kragic, T. Asfour, and N. Krger ”A strategy for grasping unknown objects based on co-planarity and colour information”, Robotics and Autonomous Systems, vol. 58(5), pp. 551-565, 2010.
[3] P. Allen ”Integrating vision and touch for object recognition tasks”, The International Journal of Robotics Research, vol. 7(6), pp. 15-33, 1988.
[4] J. Bimbo, L. Seneviratne, K. Althoefer, and H. Liu ”Combining touch and vision for the estimation of an objects pose during manipulation”, In Proc. IEEE/RSJ Int. Conf. Intell. Robots and Syst. (IROS), pp. 4021–4026, 2013.
[5] M. Bjorkman, Y. Bekiroglu, V. Hogman, and D. Kragic ”Enhancing visual perception of shape through tactile glances”, In Proc. IEEE/RSJ Int. Conf. Intell. Robots and Syst. (IROS), pp. 3180–3186, 2013.
[6] N. Lepora, K. Aquilina, and L Cramphorn ”Exploratory tactile servoing with active touch”, IEEE Robotics and Automation Letters, pp. 117–124, 2017.
[7] T. Bhattacharjee, A. Shenoi, D. Park, J. Rehg, and C. Kemp ”Combining tactile sensing and vision for rapid haptic mapping”, In Proc. IEEE/RSJ Int. Conf. Intell. Robots and Syst. (IROS), pp. 1200–1207, 2015.
[8] N. Jamali, C. Ciliberto, L. Rosasco, and L. Natale ”Active perception: Building objects models using tactile exploration”, In Proc. IEEE-RAS Int. Conf. on Humanoid Robots (Humanoids), pp. 179–185, 2016.
[9] P. Falco, S. Lu, A. Cirillo, C. Natale, S. Pirozzi and D. Lee ”Crossmodal Visuo-Tactile Object Recognition Using Robotic Active Exploration”, In Proc. IEEE Int. Conf. Robot. Autom. (ICRA), accepted, 2017.
[10] Website of the WIRES experiment, http://www-lar.deis.unibo.it/people/gpalli/WIRES/
[11] SYNDY Website, http://www.systemrobot.it/syndy-en.asp
[12] Kiesling Website, http://www.kiesling.net/en/produkte/averex-verdrahtung.php
[13] Tombari F., Franchi A., and Di Stefano L.. "BOLD features to detect texture-less objects." Proceedings of the IEEE International Conference on Computer Vision. 2013.
[14] Wires - Object Recognition Experiments, https://www.youtube.com/watch?v=OLl97pk7uZM
[15] G. De Maria, C. Natale, and S. Pirozzi ”Force/tactile sensor for robotic applications”, Sensors and Actuators A: Physical, vol. 175, pp. 6072, 2012.